



上海交通大学  
SHANGHAI JIAO TONG UNIVERSITY



李政道研究所  
Tsung-Dao Lee Institute

# Fiducial and differential cross-section measurements of $EW W\gamma jj$ production at 13TeV with the ATLAS detector

Jing Chen

2024.11.15

CLHCP2024

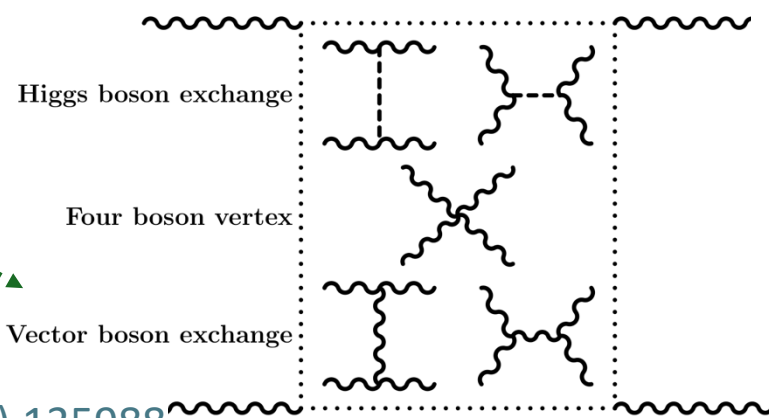
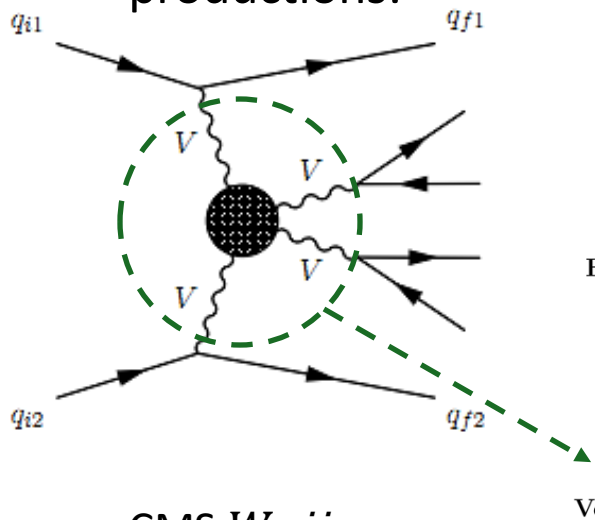
# Introduction



- **Vector boson scattering (VBS)** measurements offers an important way to probe electroweak symmetry breaking.
- Sensitive to new physics: **probe aTGC, aQGC ...**
- A good probe of the SM in the electroweak (EW) sector. Measure VBS via the corresponding EW productions.

$W\gamma jj$

- For VBS processes, many channels have been measured and observed at LHC.



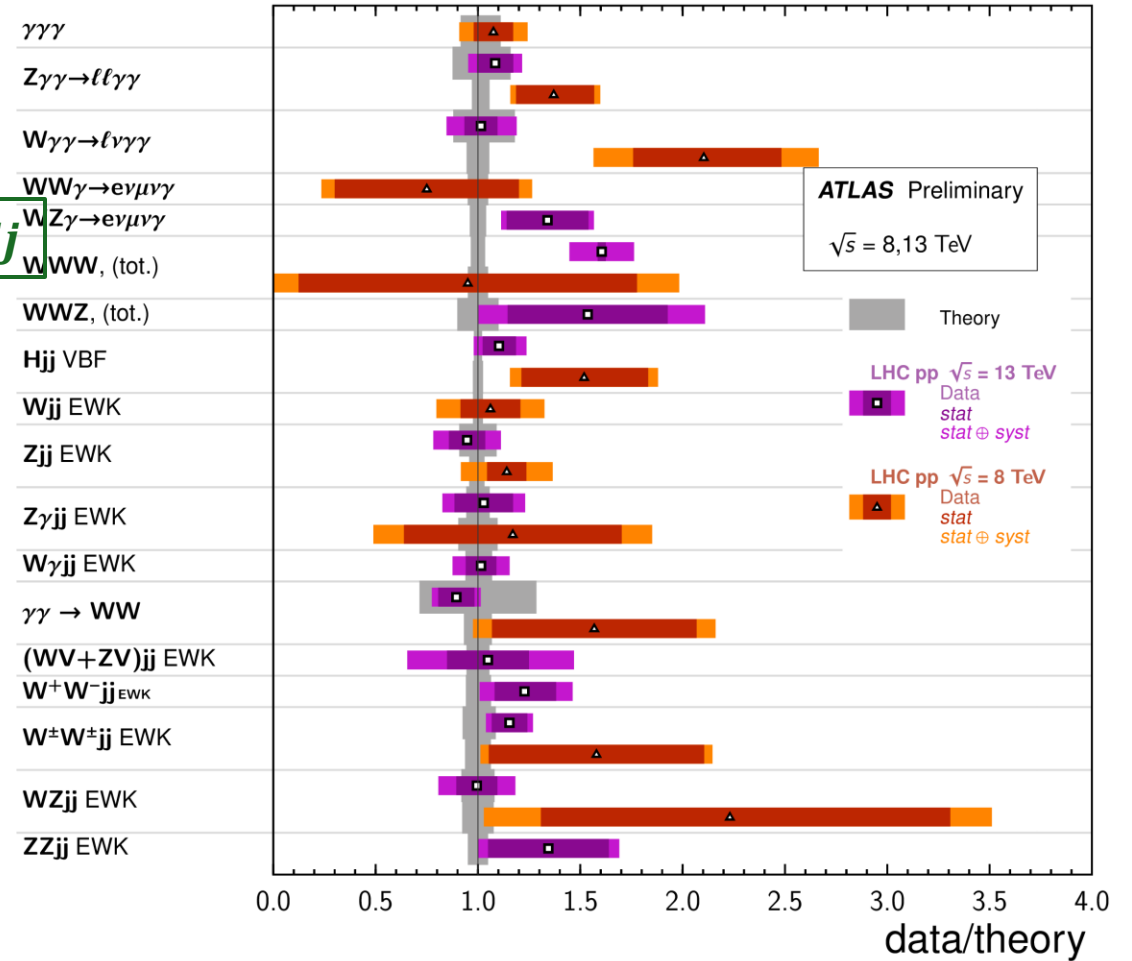
- CMS  $W\gamma jj$ :

[Phys. Lett. B 811 \(2020\) 135988](#)

[Phys. Rev. D 108 \(2023\) 032017](#)

**VBF, VBS, and Triboson Cross Section Measurements**

Status: June 2024



**1<sup>st</sup> observation of EW  $W\gamma jj$  at ATLAS.**

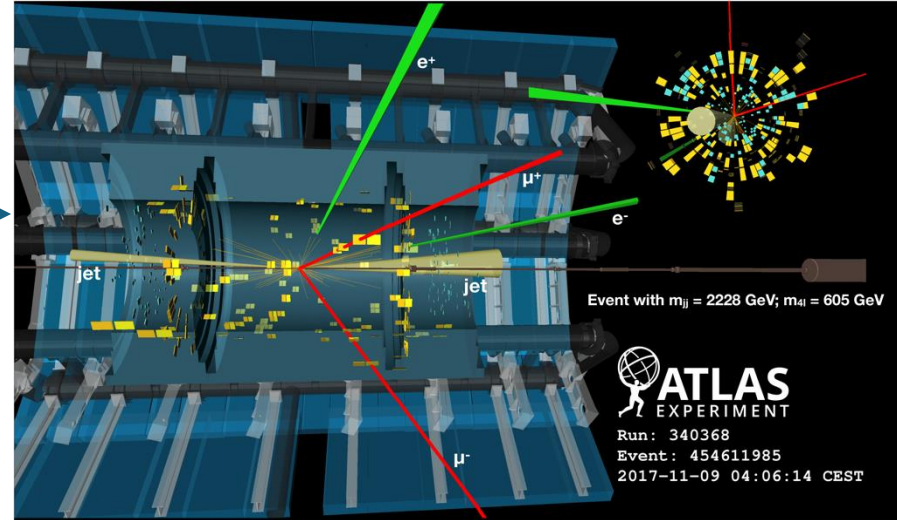
# $W\gamma jj$



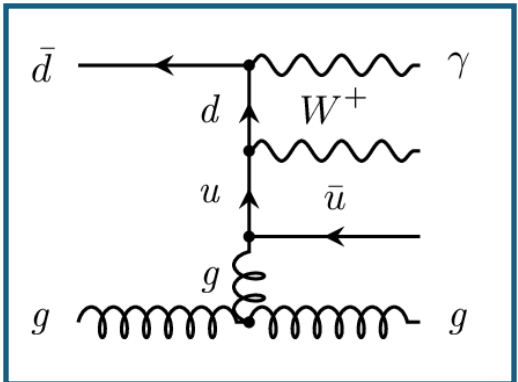
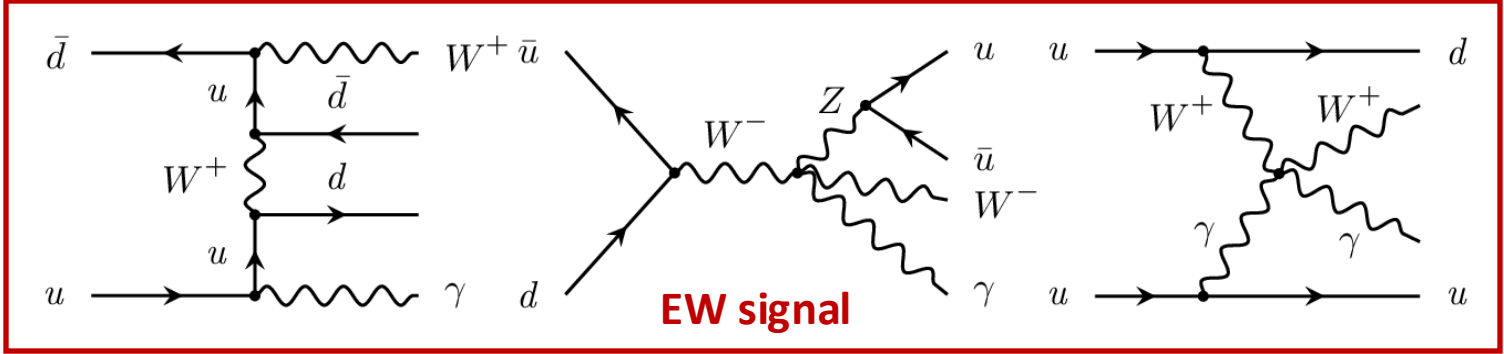
- **EW  $W(\rightarrow l\nu)\gamma jj$ :**
  - **Observation** of EW  $W\gamma jj$  production.
  - **Differential cross-section** measurements.
  - Limits on **aQGC**.
- **Full Run2 datasets ( $140 fb^{-1}$ ).**

- **VBS topology:**

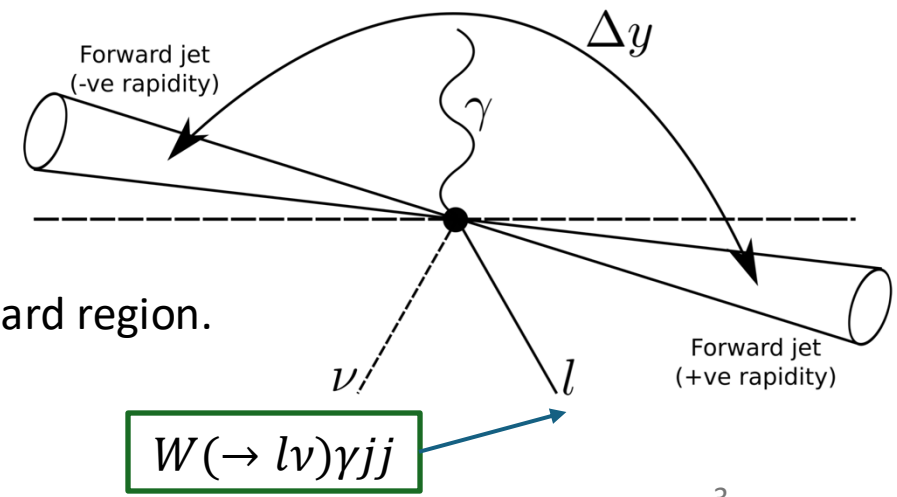
$ZZjj$



*Nature Physics 19 (2023) 237-253*



- Perform measurement in **VBS-enhanced** phase space.
  - two energetic jets in the forward and backward region.
  - High  $m_{jj}$ , large  $\Delta y_{jj}$ .





- **Observation and fiducial cross section measurement**

- A control region (CR) is defined to constrain the QCD background.
- Data driven method is used to estimate all non-prompt, fake, pileup backgrounds.
- Fit the Neural Network (NN) output to extract the signal strength ( $\mu_{EW}$ ).
- Fiducial cross-section is obtained by correcting the detector effects.

- **Differential cross section measurement**

- Three CRs are defined to constrain QCD background.

$$\Delta\phi_{jj} = \phi_f^j - \phi_b^j \leftarrow y_f^j > y_b^j$$

- Observables:  $m_{jj}, p_T^{jj}, p_T^l, m_{l\gamma}$  (VBS observables, sensitive to aQGC),  $\Delta\phi_{jj}, \Delta\phi_{l\gamma}$  (Charge conjugation and Parity observables, probe CP structure).

$$\Delta\phi_{l\gamma} = \phi_f - \phi_b \leftarrow y_f > y_b$$

- EFT interpretation: The six unfold observable distributions are used to constrain dimension-8 (D-8) operators (sensitive to quartic gauge couplings).

# Object & event selection



- object selection:**

$\gamma$	lepton	Jets
<ul style="list-style-type: none"> <li>- At least 1 tight and isolated <math>\gamma</math>.</li> <li>- <math>p_T &gt; 22</math> GeV.</li> <li>- <math> \eta  &lt; 2.37</math>.</li> </ul>	<ul style="list-style-type: none"> <li>- 1 tight and isolated lepton.</li> <li>- <math>p_T &gt; 30</math> GeV.</li> <li>- <math> \eta  &lt; 2.5</math>.</li> <li>- 2<sup>nd</sup> lepton veto.</li> </ul>	<ul style="list-style-type: none"> <li>- At least 2 jets.</li> <li>- <math>p_T &gt; 50</math> GeV.</li> <li>- <math> \eta  &lt; 4.4</math>.</li> <li>- No b-jets (DL1r at 85%WP)</li> </ul>

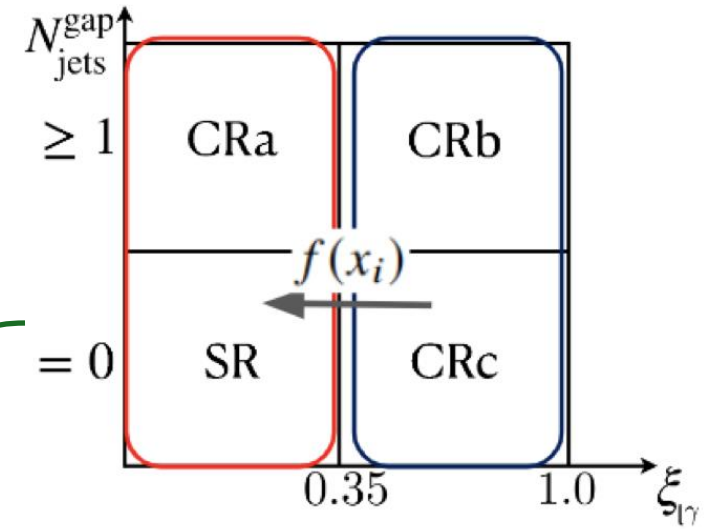
- Event selection:**

- $m_T^W > 30$  GeV.
- $E_T^{miss} > 30$  GeV.
- $|m_{l\gamma} - m_Z| > 10$  GeV.
- Standard object overlap removal.

Observation & fiducial cross-section

SR	CR
$\Delta y_{jj} > 2, m_{jj} > 500$ GeV	
$N_{jets}^{gap} = 0$	$N_{jets}^{gap} > 0$

$$\xi_{l\gamma} = \left| y_{l\gamma} - \frac{(y_{j1} + y_{j2})}{2} / (y_{j1} - y_{j2}) \right|$$



Differential cross-section

$N_{jets}^{gap}$ : Number of jets in rapidity gap  $\Delta y$ .

+

$\Delta y_{jj} > 2$   
 $m_{jj} > 1000$  GeV

# Background estimation



- **QCD background:**

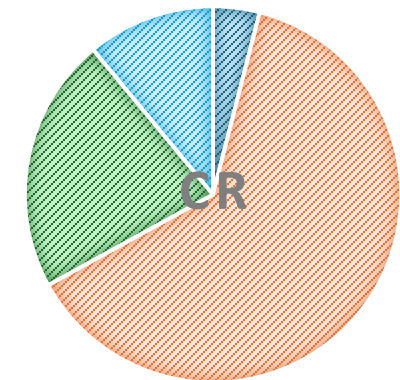
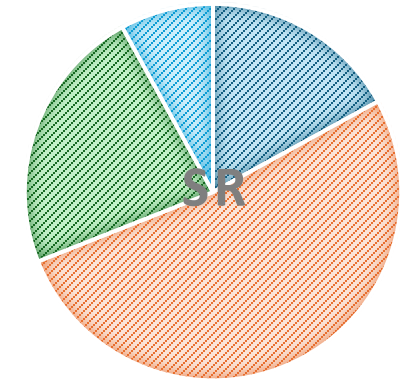
- Main background.
- Strong  $W\gamma jj$ .
- A control region is defined to constrain the QCD background.
- Simultaneously fit the NN output in signal region and control region.

- **Prompt background:**

- Top +  $Z\gamma jj$ .
- Estimate by using MC simulation.

- **Non-prompt background:**

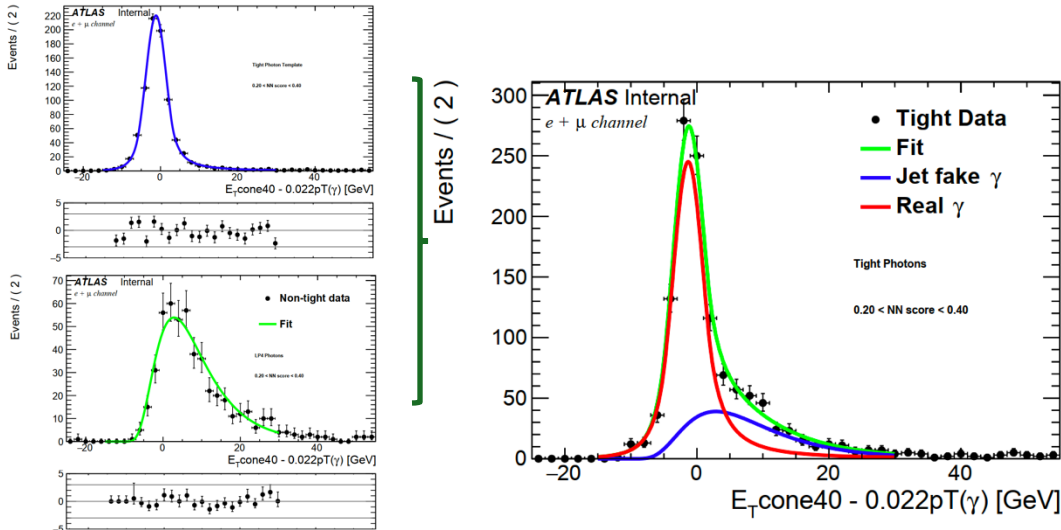
- **Jet fake photon:** Largest non-prompt background (W+jet). A data-driven **template fit** is used.
- **Jet fake lepton:** Leptons arising from mis-reconstructed jets or in-flight decays of hadrons. **Fake factor** method is used.
- **Electron fake photon:** Arise from conversions and inefficient calorimeter to track matching (Z+jets &  $t\bar{t}$ ). **Tag & probe** method is used.
- **Pile-up photon:** A photon originating from one  $pp$  interaction is selected alongside a Wjj event from another  $pp$  interaction from the same bunch crossing. Data driven method is used.



# Background estimation



## • Jet fake photon:



- Prompt  $\gamma$  isolation shape  $\leftarrow$  tight ID  $\gamma$ .
- Non-prompt  $\gamma$  isolation shape  $\leftarrow$  non-tight ID  $\gamma$ .
- Uncertainties: Stat. uncertainty in template & fit, choice of  $\gamma$  ID criteria, real  $\gamma$  subtraction,  $E_T^{iso,\gamma}$  modelling.
- ABCD method is used to cross check.

## • Jet fake lepton:

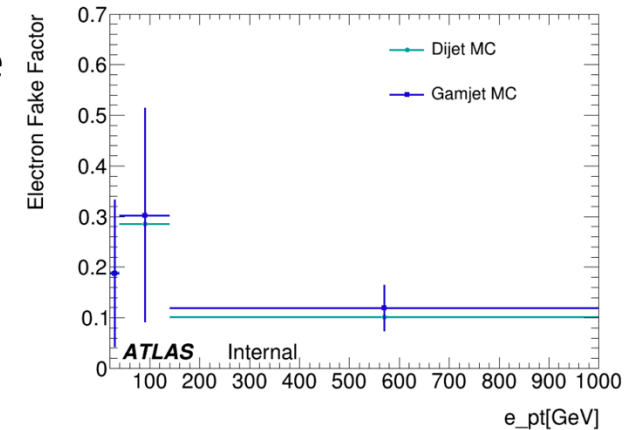
Fake efficiency: 
$$\epsilon = \frac{N_e^{tight}}{N_e^{loose}}$$

Fake factor: 
$$F = \frac{\epsilon}{1 - \epsilon}$$

Fake lepton background in SR:

$$N_{fakelep} = F_{e/\mu} \times (N_{e/\mu-data}^{anti-tight} - N_{e/\mu-prompt-lepton}^{anti-tight})$$

- Dijet sample is used to get fake factors. A closure test has performed between dijet and gamjet samples.
- Fake factor with different  $p_T$  and  $\eta$  bins are measured.
- Uncertainties: Stat., jet composition uncertainty ( $\gamma$  + jet vs dijet), variation of selection cuts, prompt lepton subtraction with different QCD MC samples, variation of  $p_T$ ,  $\eta$  binning of fake factor, background subtraction in dijet region.



# Background estimation



- **Electron fake photon:**

- Fake and real enriched regions defined by the presence of a probe electron or a probe photon.

- Fake rate:

$$F_{e \rightarrow \gamma} = \frac{N_{\gamma}^{reco} \epsilon_{\gamma}}{N_e^{reco} \epsilon_e}$$

$\epsilon_{\gamma}, \epsilon_e$ : the identification efficiency for  $\gamma$  and e.

- uncertainties: Stat., variation of fit range, integration range,  $p_T, \eta$  binning, different fit function in the fit.

- **Pile-up photon**

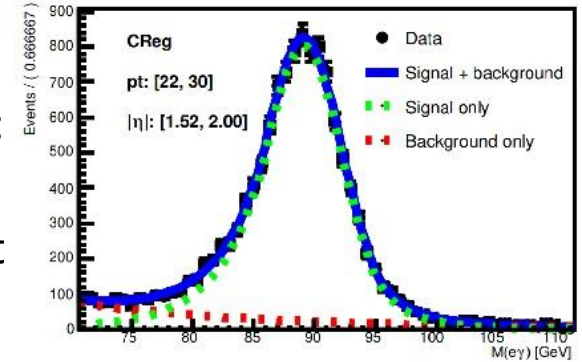
Pile-up fraction:

$$f_{PU} = \frac{N_{data}^{|\Delta z| > 50mm} - N_{MC}^{|\Delta z| > 50mm}}{N_{data} * 0.32} * C$$

C is a normalization factor derived by comparing the MC to data.

- Only converted photons with hits in the silicon tracker are used to ensure good resolution.
- Real photon purity is applied to fake fraction to avoid double counting pileup jets with fake photons.
- $f_{pu} = (1.7 \pm 1.6)\%$  in SR.

- Estimated under Z peak:  $|M_Z - M_{e\gamma}| < 10$  using a signal + background fit



$$F_{e \rightarrow \gamma} = \frac{N_{e\gamma}}{2N_{ee}} = \frac{S_{e\gamma} + B_{e\gamma}}{2(S_{ee} + B_{ee})} = \frac{S_{e\gamma} + S_{e\gamma}(\frac{1}{S/B})}{2(S_{ee} + S_{ee}(\frac{1}{S/B}))} = \frac{S_{e\gamma} (1 + \frac{1}{S/B})}{2S_{ee} (1 + \frac{1}{S/B})} = \frac{S_{e\gamma}}{2S_{ee}}$$

- **Event yields:**

	SR <sup>fid</sup> ( $N_{jets}^{gap} = 0$ )	CR <sup>fid</sup> ( $N_{jets}^{gap} > 0$ )
EW $W\gamma jj$	520 ± 141	120 ± 49
Strong $W\gamma jj$	1550 ± 830	1970 ± 950
Non-prompt	692 ± 57	698 ± 58
Top quark processes	109 ± 18	183 ± 37
EW + strong $Z\gamma jj$	128 ± 34	163 ± 77
Total	3000 ± 830	3140 ± 960
Data	3341	3143



# Observation & fiducial cross-section



- **Signal extraction:**

- Simultaneously fit the NN output in signal region and control region.
- Two floating normalization factors:  $\mu_{EW}$  &  $\mu_{strong}$ .

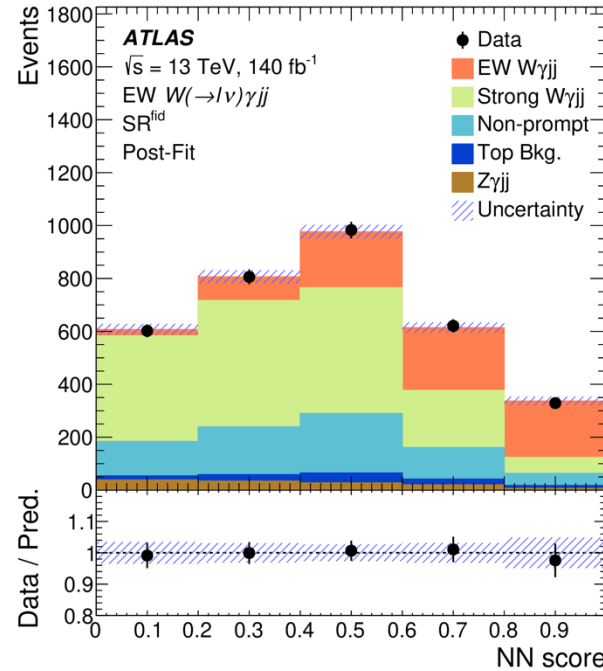
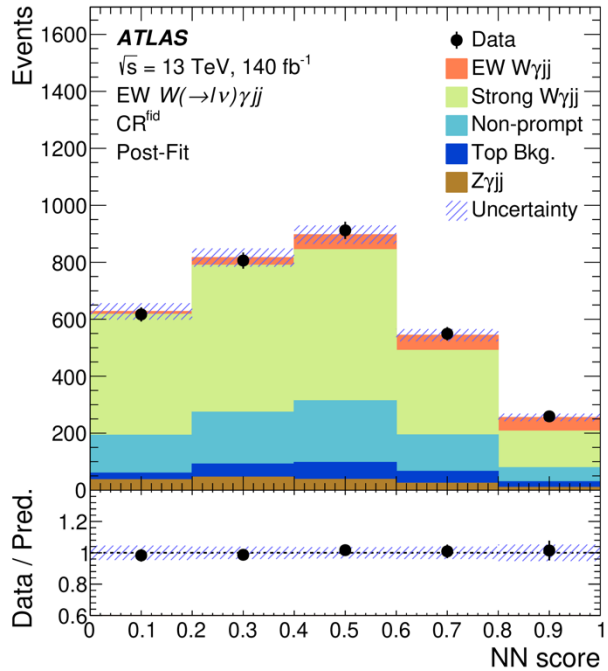
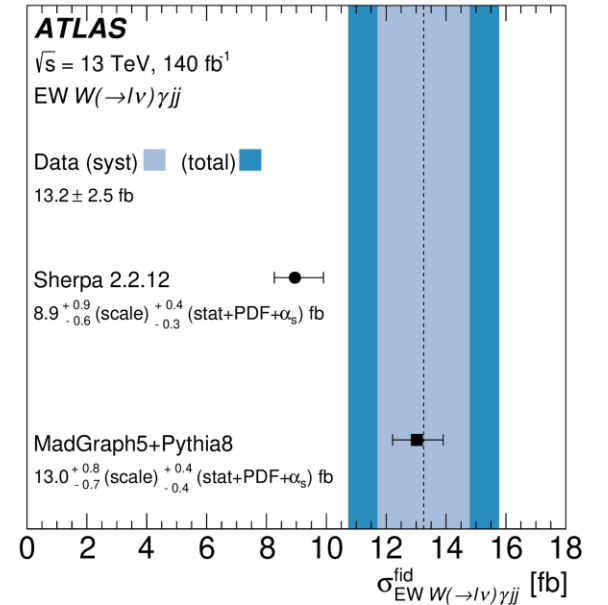
- **Observation:**

- $\mu_{EW} = 1.5 \pm 0.5$ .
- Observed (expected) significance:  **$9.0\sigma$**  ( **$6.3\sigma$** ) **1<sup>st</sup> observation at ATLAS!**

- **Fiducial cross-section:**

$$\sigma_{EW W\gamma jj}^{fid} = \frac{N_{EW W\gamma jj}}{L \cdot C_{EW W\gamma jj}}$$

$$C_{EW W\gamma jj} = \frac{N_{reco.}}{N_{fid.}}$$



Uncertainty Source	Fractional Uncertainty [%]
MC Statistics	11
Jets	8
Lepton, photon, pile-up	8
EW $W\gamma jj$ modelling	7
Data Statistics	6
Strong $W\gamma jj$ modelling	6
Non-prompt background	2
Luminosity	2
Other Background modelling	2
$E_T^{miss}$	1

**Dominant** (points to MC Statistics)

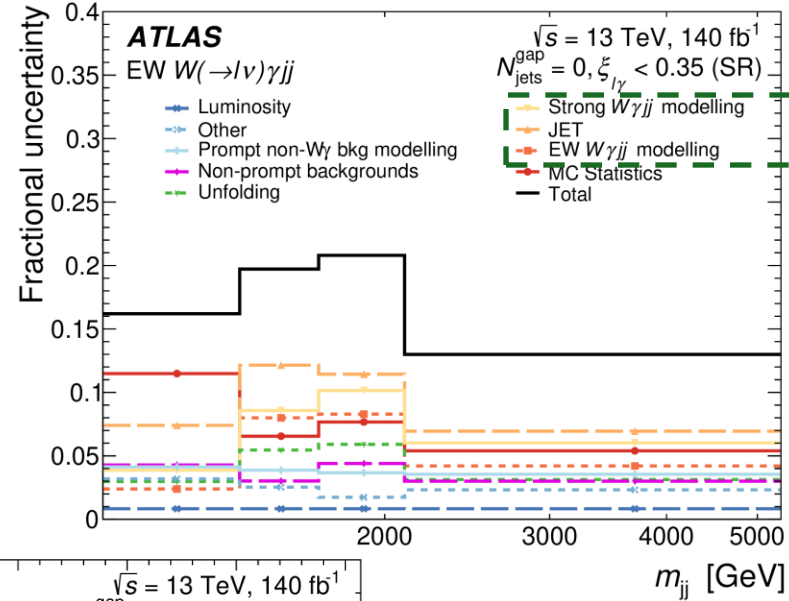
**Large JES & JER** (points to Jets and Lepton, photon, pile-up)

# Differential cross-section

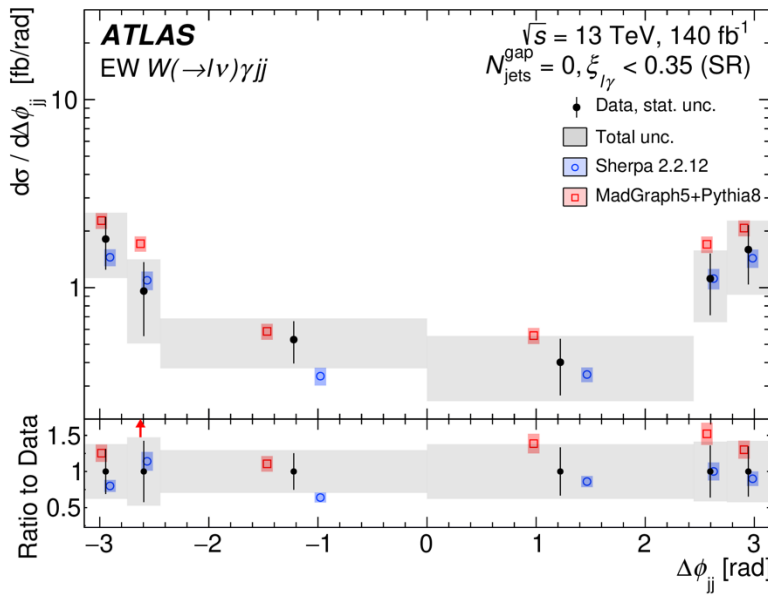
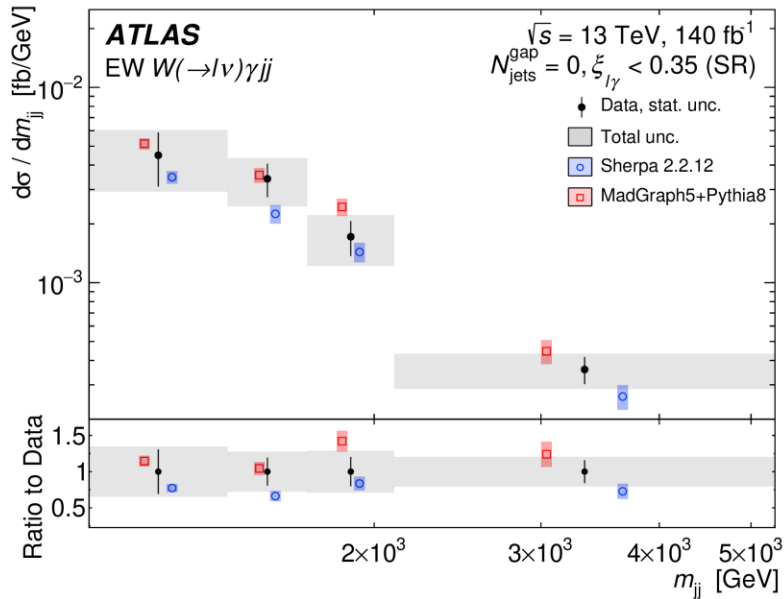


- **Signal extraction:**

- SR + 3CRs: defined by  $N_{jets}^{gap}$  &  $\xi_{l\gamma}$ .
- Observables:  $m_{jj}, p_T^{jj}, p_T^l, m_{l\gamma}, \Delta\phi_{jj}, \Delta\phi_{l\gamma}$ .
- Simultaneously fit in signal and control regions with bin by bin reweighting of signal and QCD components in each region.
- The extracted yields are unfolded to produce differential cross sections.



Dominated uncertainties



- **Differential cross-section:**

- The predictions from both MadGraph5+Pythia8 and Sherpa are in agreement with the data within uncertainties.

# EFT interpretation



- The effective Lagrangian:

$$\mathcal{L}_{\text{eff}} = \mathcal{L}_{\text{SM}} + \sum_j \frac{f_j^{(8)}}{\Lambda^4} O_j^{(8)}$$

Wilson coefficients      dimension-8 operators  
energy scale of new physics

- The differential cross-section can be decomposed into 3 terms:

$$|\mathcal{M}|^2 = |\mathcal{M}_{\text{SM}}|^2 + 2\text{Re}(\mathcal{M}_{\text{SM}}^* \mathcal{M}_{\text{D-8}}) + |\mathcal{M}_{\text{D-8}}|^2$$

scales linearly w/  $f_j^{(8)}$   
scales quadratically w/  $f_j^{(8)}$

- $W\gamma jj$ :

- Sensitive to potential anomalous quartic couplings of  $WW\gamma\gamma$  &  $WW\gamma Z$ .
- $p_T^{jj}$  (most sensitive to tensor-type operators),  $p_T^l$  (most sensitive to mixed-scalar operators).
- Constraints on the  $f_{T3}$  and  $f_{T4}$  operators: **1<sup>st</sup> such limits at the LHC.**

Coefficients [TeV <sup>-4</sup> ]	Observable	$M_{W\gamma}$ cut-off [TeV]	Expected [TeV <sup>-4</sup> ]	Observed [TeV <sup>-4</sup> ]
$f_{T0}/\Lambda^4$	$p_T^{jj}$	-	[-2.4,2.4]	[-1.7,1.8]
$f_{T1}/\Lambda^4$	$p_T^{jj}$	-	[-1.5,1.6]	[-1.1,1.2]
$f_{T2}/\Lambda^4$	$p_T^{jj}$	-	[-4.4,4.7]	[-3.1,3.5]
$f_{T3}/\Lambda^4$	$p_T^{jj}$	-	[-3.3,3.5]	[-2.4,2.6]
$f_{T4}/\Lambda^4$	$p_T^{jj}$	-	[-3.0,3.0]	[-2.2,2.2]
$f_{T5}/\Lambda^4$	$p_T^{jj}$	1.1	[-9.9,9.9]	[-7.5,7.5]
$f_{T6}/\Lambda^4$	$p_T^{jj}$	1.3	[-7.4,7.6]	[-5.2,5.4]
$f_{T7}/\Lambda^4$	$p_T^{jj}$	-	[-3.8,3.9]	[-2.7,2.8]
$f_{M0}/\Lambda^4$	$p_T^l$	-	[-38,37]	[-38,37]
$f_{M1}/\Lambda^4$	$p_T^l$	-	[-57,58]	[-41,42]
$f_{M2}/\Lambda^4$	$p_T^l$	0.8	[-110,110]	[-88,82]
$f_{M3}/\Lambda^4$	$p_T^l$	1.1	[-100,110]	[-73,77]
$f_{M4}/\Lambda^4$	$p_T^l$	1.0	[-118,111]	[-89,83]
$f_{M5}/\Lambda^4$	$p_T^l$	1.3	[-57,80]	[-32,77]
$f_{M7}/\Lambda^4$	$p_T^l$	-	[-96,95]	[-69,68]

Coefficients [TeV <sup>-4</sup> ]	Observable	Expected [TeV <sup>-4</sup> ]	Observed [TeV <sup>-4</sup> ]
$f_{T0}/\Lambda^4$	$p_T^{jj}$	[-2.4, 2.4]	[-1.8, 1.8]
$f_{T1}/\Lambda^4$	$p_T^{jj}$	[-1.5, 1.6]	[-1.1, 1.2]
$f_{T2}/\Lambda^4$	$p_T^{jj}$	[-4.4, 4.7]	[-3.1, 3.5]
$f_{T3}/\Lambda^4$	$p_T^{jj}$	[-3.3, 3.5]	[-2.4, 2.6]
$f_{T4}/\Lambda^4$	$p_T^{jj}$	[-3.0, 3.0]	[-2.2, 2.2]
$f_{T5}/\Lambda^4$	$p_T^{jj}$	[-1.7, 1.7]	[-1.2, 1.3]
$f_{T6}/\Lambda^4$	$p_T^{jj}$	[-1.5, 1.5]	[-1.0, 1.1]
$f_{T7}/\Lambda^4$	$p_T^{jj}$	[-3.8, 3.9]	[-2.7, 2.8]
$f_{M0}/\Lambda^4$	$p_T^l$	[-28, 28]	[-24, 24]
$f_{M1}/\Lambda^4$	$p_T^l$	[-43, 44]	[-37, 38]
$f_{M2}/\Lambda^4$	$p_T^l$	[-10, 10]	[-8.6, 8.5]
$f_{M3}/\Lambda^4$	$p_T^l$	[-16, 16]	[-13, 14]
$f_{M4}/\Lambda^4$	$p_T^l$	[-18, 18]	[-15, 15]
$f_{M5}/\Lambda^4$	$p_T^l$	[-17, 14]	[-14, 12]
$f_{M7}/\Lambda^4$	$p_T^l$	[-78, 77]	[-66, 65]

# Summary



- **1<sup>st</sup> observation** of EW  $W\gamma jj$  at ATLAS.
  - $\mu_{EW} = 1.5 \pm 0.5$ .
  - Observed (expected) significance:  **$9.0\sigma$  ( $6.3\sigma$ )**.
- Measurements of EW  $W\gamma jj$  **fiducial** and **differential cross-section** are reported.
  - $\sigma_{EW}^{fid} = 13.2 \pm 2.5 fb$ .
  - **Differential cross-sections are measured** as functions of six kinematic observables.
  - The data are corrected for detector effects of inefficiency and resolution using an iterative Bayesian **unfolding** method.
  - These differential measurements are used to **search for anomalous quartic boson interactions** using D-8 operators in the context of an effective field theory.
  - The first LHC constraints on  $f_{T3}$  and  $f_{T4}$  are presented.
- Publication: [Eur. Phys. J. C 84 \(2024\) 1064](#)



上海交通大學

SHANGHAI JIAO TONG UNIVERSITY

谢谢!

# Particle level definition



Object	Selection requirements
Dressed muons	$p_T > 30 \text{ GeV}$ and $ \eta  < 2.5$
Dressed electrons	$p_T > 30 \text{ GeV}$ and $ \eta  < 2.47$ (excluding $1.37 <  \eta  < 1.52$ )
Isolated photons	$E_T^\gamma > 22 \text{ GeV}$ and $ \eta  < 2.37$ (excluding $1.37 <  \eta  < 1.52$ ) and $E_T^{\text{iso}} < 0.2E_T^\gamma$
Jets	At least two jets with $p_T > 50 \text{ GeV}$ and $ y  < 4.4$ , $b$ -jet veto
Missing transverse momentum	$E_T^{\text{miss}} > 30 \text{ GeV}$ and $m_T^W > 30 \text{ GeV}$
VBS topology	$N_\ell = 1, N_\gamma \geq 1,  m_{\ell\gamma} - m_Z  > 10 \text{ GeV}$ $\Delta R_{\min}(\ell, j) > 0.4, \Delta R_{\min}(\gamma, j) > 0.4, \Delta R_{\min}(\ell, \gamma) > 0.4$ $\Delta R_{\min}(j_1, j_2) > 0.4, \Delta\phi_{\min}(E_T^{\text{miss}}, j) > 0.4$ $N_{\text{jets}} \geq 2, p_T^{j1}, p_T^{j2} > 50 \text{ GeV}$ $m_{jj} > 500 \text{ GeV},  \Delta y_{jj}  > 2$
Fiducial measurement	VBS topology
Differential measurement	VBS topology $\oplus (m_{jj} > 1000 \text{ GeV}, N_{\text{jets}}^{\text{gap}} = 0, \text{ and } \xi_{W\gamma} < 0.35)$

# MC samples



Signal. Sh-2.2.11 Nominal, MG5 systematic

Irreducible bkg. Sh-2.2.11 Nominal, MG5 systematic

Reducible prompt bkg.

Non-prompt backgrounds used for DD fakes estimates

Process	Prompt/Non-prompt	Generator	ME Accuracy	PDF	Shower & Hadronization	Parameter Tune
EW $W\gamma jj$	Prompt	Madgraph5	LO	NNPDF3.1 LO	Pythia8+EvtGen	A14
		Sherpa 2.2.12	LO	NNPDF3.0 NLO	Sherpa	Default
QCD $W\gamma jj$	Prompt	Sherpa 2.2.11	NLO	NNPDF3.0 NLO	Sherpa	default
		Madgraph5	NLO	NNPDF3.0 NLO	Pythia8+EvtGen	A14
EW $Z\gamma jj$	Prompt	Madgraph5	LO	NNPDF3.1 LO	Pythia8+EvtGen	A14
QCD $Z\gamma jj$	Prompt	Sherpa 2.2.11	NLO	NNPDF3.0 NLO	Sherpa	default
$t\bar{t}\gamma$	Prompt	Madgraph5	LO	NNPDF2.3 LO	Pythia8+EvtGen	A14
$tW\gamma$	Prompt	Madgraph5	LO	NNPDF3.0 NLO	Pythia8+EvtGen	A14
$tq\gamma$	Prompt	Madgraph5	LO	NNPDF3.0 NLO	Herwig7+EvtGen	Default
Single Top	Prompt	Powheg	NLO	NNPDF3.0 NLO	Pythia8+EvtGen	A14
W+jets	Non-Prompt	Sherpa 2.2.11	NLO	NNPDF3.0 NNLO	Sherpa	Default
Z+jets	Non-Prompt	Sherpa 2.2.11	NLO	NNPDF3.0 NNLO	Sherpa	Default
Diboson	Non-Prompt	Sherpa 2.2.12	NLO	NNPDF 3.0 NNLO	Sherpa	Default
Dijet	Non-Prompt	Pythia8	LO	NNPDF2.3 LO	Pythia8+EvtGen	A14
EW $Wjj$	Non-Prompt	Sherpa 2.2.1	LO	NNPDF3.0 NNLO	Sherpa	default
EW $Zjj$	Non-Prompt	Sherpa 2.2.1	LO	NNPDF3.0 NNLO	Sherpa	default
$t\bar{t}$	Non-Prompt	Powheg	NLO	NNPDF3.0 NLO	Pythia8+EvtGen	A14
$tW$	Non-Prompt	Powheg	NLO	NNPDF3.0 NLO	Pythia8+EvtGen	A14

# MadGraph & Sherpa signal comparison



- The difference certainly comes from having the **3rd jet included in the matrix element in Sherpa**.
- Diagrams with gluon emission from the incoming or outgoing quarks interfere destructively, resulting in a suppression of centrally produced jets. ([More details](#))
- Sherpa sample predicts more hadronic activity in the gap between the two leading jets.

$$\eta_{j3}^* = \eta_{j3} - \frac{\eta_{j1} + \eta_{j2}}{2}$$

